Correlated, Dual-Beam Optical Gating in Coupled Organic–Inorganic Nanostructures

Wurst, Kai M.; Bender, Markus; Lauth, Jannika; Maiti, Sonam; Chassé, Thomas; Meixner, Alfred; Siebbeles, Laurens D.A.; Bunz, Uwe H.F.; Braun, Kai; Scheele, Marcus

DOI
10.1002/anie.201803452

Publication date
2018

Document Version
Final published version

Published in
Angewandte Chemie - International Edition

Conductive Polymers

International Edition: DOI: 10.1002/anie.201803452
German Edition: DOI: 10.1002/ange.201803452

Correlated, Dual-Beam Optical Gating in Coupled Organic–Inorganic Nanostructures

Kai M. Wurst, Markus Bender, Jannika Lauth, Sonam Maiti, Thomas Chassé, Alfred Meixner, Laurens D. A. Siebbeles, Uwe H. F. Bunz, Kai Braun, and Marcus Scheele**

Abstract: *An optical switch with two distinct resonances is formed by combining PbS nanocrystals and the conductive polymer poly[sodium 2-(2-ethynyl-4-methoxyphenoxy)acetate] (PAE) into a hybrid thin film. Infrared excitation of the nanocrystals invokes charge transfer and consecutive polaron formation in the PAE, which activates the switch for excited-state absorption at visible frequencies. The optical modulation of the photocurrent response of the switch exhibits highly wavelength-selective ON/OFF ratios. Transient absorption spectroscopy shows that the polaron formation is correlated with the excited state of the nanocrystals, opening up new perspectives for photonic data processing. Such correlated activated absorption can be exploited to enhance the sensitivity for one optical signal by a second light source of different frequency as part of an optical amplifier or a device with AND logic.*

Optical switches are key components for data processing on the basis of silicon photonics, where they perform the crucial conversion of a photonic signal from an optical fiber into an electric signal for a silicon-based processing unit.[1,2] The switch is controlled by an external light source, emitting light at a wavelength in the absorption envelope of a conductive channel to photo-induce additional charge carriers. This action modulates the current output of the switch in close analogy to a classic transistor.[3] Currently applied optical switches are mostly based on Ge or InP, but better alternatives in terms of materials and/or device architectures are highly desirable[1,4] These efforts include attempts to replace Ge or InP with two-dimensional semiconductors, organic electro-optical materials, or inorganic semiconductor nanocrystals (NC).[5–7] While organic optical switches display impressive photocurrent on/off ratios of $>10^5$, a key challenge is to find materials with high absorption at telecommunication wavelengths (1260–1625 nm) and sufficient photostability.[8] In contrast, these conditions are often fulfilled by NCs, however the high sensitivity to surface defects has limited the ON/OFF ratios of purely NC-based optical switches to about 10^3.[9–11] This has inspired the exploration of hybrid optical switches to combine the benefits of organic semiconductors and NCs in a single material.[12–14] Upon combination of semiconductor NCs and conjugated polymers a variety of charge- and energy-transfer processes emerge under optical excitation, which render these materials attractive as optical switches.[15]

Herein, we report a hybrid optical switch composed of PbS NCs and poly[sodium 2-(2-ethynyl-4-methoxyphenoxy)acetate] (PAE-**1**; for the structural formula, see the Supporting Information) and focus on the wavelength-selective photoresponse. We find that IR-excitation of the NCs creates a polaron in PAE-**1**, which activates the absorption of visible light. We argue that such activated absorption enables complex logic operations within a single optical switch, such as processing two optical signals simultaneously.

Hybrid thin films of PbS NCs cross-linked with PAE-**1** were assembled as floating membranes at the acetonitrile/N_2 interface and coated onto solid supports (see the Supporting Information, Figure S1 for Raman spectroscopy).[16] Figure 1 a displays the transconductance of two films of different thicknesses. 30–40 nm thin films exhibit near-ambipolar behavior with mobilities of $0.5–1.0\times10^{-3}\,cm^2\,V^{-1}\,s^{-1}$, carrier concentrations of about $10^{14}\,cm^{-3}$ and an ON/OFF ratio of about 10^5 (see the Supporting Information, Figure S2 for the height profile). Thicker films (> 50 nm) show a reduced ON/OFF ratio of 2–3 orders of magnitude, mobilities of about $1\times10^{-2}\,cm^2\,V^{-1}\,s^{-1}$ and carrier concentrations of $0.5–1.0\times10^{16}\,cm^{-3}$. The favorable ON/OFF ratios of the thin films led us to investigate their photophysical properties towards optical gating with a 638 nm Laser diode. Note that photons of this energy cannot excite PAE-**1** directly. Figure 1 b depicts the semi-logarithmic response of the film to optical excitation at this wavelength with an absorbed optical power $\leq35\,\mu W$ and two different source/drain voltages (V_{SD}). At $V_{SD}=-6$ V, the maximum ON/OFF ratio between dark current and photocurrent is about 2800 with a responsivity of about $20\,mA\,W^{-1}$, while at $V_{SD}=0.7$ mV we find about 1800 and

[*] K. M. Wurst, S. Maiti, Prof. T. Chassé, Prof. A. Meixner, Dr. K. Braun, Dr. M. Scheele
Institute of Physical and Theoretical Chemistry
University of Tübingen
Auf der Morgenstelle 18, 72076 Tübingen (Germany)
E-mail: marcus.scheele@uni-tuebingen.de
Dr. M. Bender, Prof. U. H. F. Bunz
Institute of Organic Chemistry and Centre for Advanced Materials
Ruprecht-Karls-Universität Heidelberg
Im Neuenheimer Feld 225, 69120 Heidelberg (Germany)
E-mail: uwe.bunz@oci.uni-heidelberg.de
Prof. L. D. A. Siebbeles
Chemical Engineering, Delft University of Technology
Van der Maasweg 9, 2629 HZ Delft (The Netherlands)
Dr. J. Lauth
Institute of Chemistry, Physical Chemistry
Carl von Ossietzky University Oldenburg
Carl-von-Ossietzky-Str. 9–11, 26129 Oldenburg (Germany)
Supporting information and the ORCID identification number(s) for the author(s) of this article can be found under: https://doi.org/10.1002/anie.201803452.

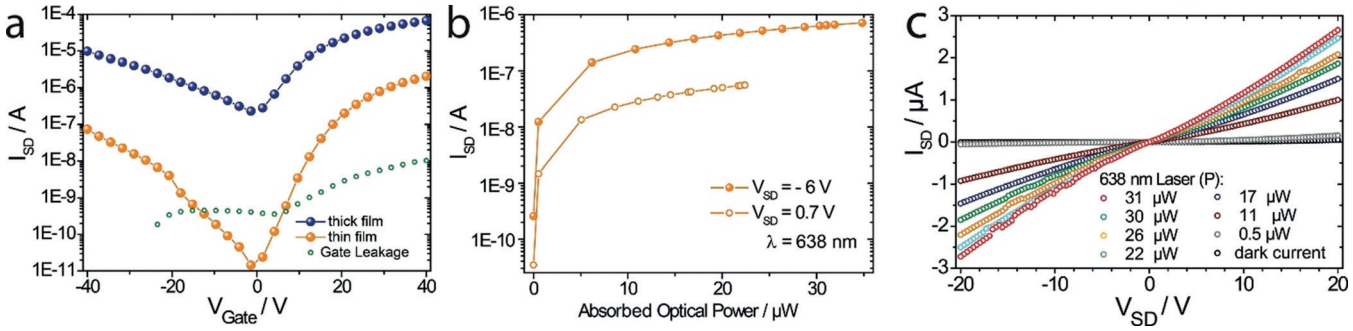

Figure 1. a) Transconductance of thin (30–40 nm, orange) and thick (> 50 nm, blue) PbS-PAE-**1** films. All of the measurements were performed in the dark. Green dots display the current leakage through the gate. b) Zero-gate photocurrent measurements of thin PbS-PAE-**1** at two different biases as a function of the absorbed optical power provided by a 638 nm laser diode. c) Current–voltage curves at different absorbed optical power values provided by a 638 nm laser diode.

about 2.5 mAW^{-1}, respectively. Responsivity is largely dependent on whether a photodetector exhibits significant gain, for instance owing to minority carrier trapping. In such cases, the responsivity can be many orders of magnitude larger, however at the cost of slow response times.[7,17,18] However, we focus here on increasing optical modulation in NC-based materials, and in this respect our room temperature ON/OFF ratios compare favorably to other recently reported NC-based optical switches.[9,11,16,19] We demonstrate this with the source-drain sweeps in Figure 1 c, which exhibit the characteristics of a moderately modulating field-effect transistor, but with an optical rather than a dielectric gate. The photocurrent spectrum of NC-based photodetectors typically resembles the absorption spectrum of the constituting NCs.[6,7,9,12,14,17,19,20] To verify this for our measurement conditions, we fabricate a reference sample from the same PbS NCs but without cross-linking with PAE-**1**. We excite the sample with the same optical power at 638 nm or 848 nm, respectively, to record the photocurrent (I_{Photo}) for each wavelength. We find a ratio of $I_{photo,638\,nm}:I_{photo,847\,nm} = 1.6 \pm 0.3$. This is in reasonable agreement with the ratio of the optical densities of the sample at 638 nm and 848 nm, which we determine as

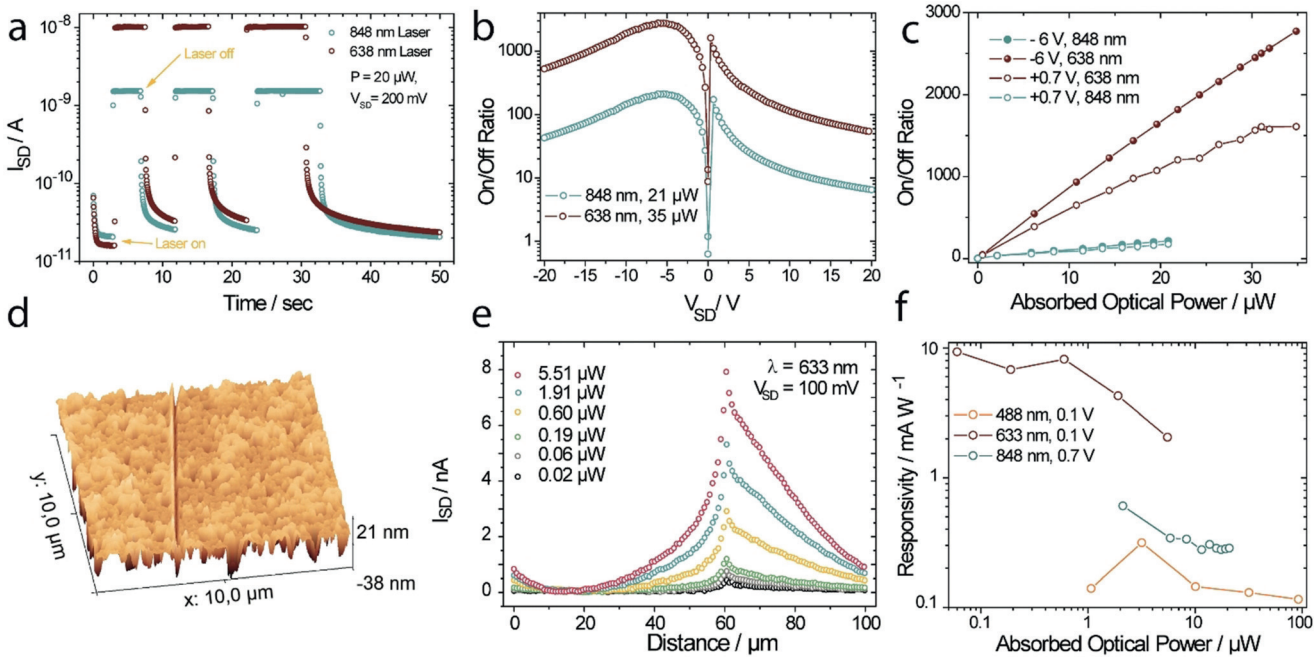

Figure 2. a) Photocurrent response of PbS-PAE-**1** upon exposure to 638 nm and 847 nm light with 20 μW absorbed optical power at a bias of +200 mV. Yellow arrows mark the instance of switching on/off the laser light. Note: the temporal response is limited here by the time constant of the source-measurement unit and no conclusions about the response time of the material can be drawn. b) ON/OFF ratio for the same PbS-PAE-1 film under 638 nm and 847 nm excitation as a function of the device bias, displaying two relative maxima at +0.7 V and −6.0 V. c) ON/OFF ratio at the two relative maxima for both excitation sources as a function of the absorbed optical power. d) Atomic force micrograph of a PbS-PAE-**1** film across a 140 nm × 100 μm trench (vertical line in the center of the micrograph). e) Line cuts through the spatially resolved confocal micrograph of the area displayed in the Supporting Information, Figure S6 under illumination with a 633 nm laser with different absorbed optical power values (See the Supporting Information, Figure S7 for the analogous measurement at 488 nm). f) Responsivities of PbS-PAE-**1** thin films as a function of absorbed optical power for 488 nm, 633 nm and 847 nm excitation.

$OD_{638\,nm}$:OD_{847nm} = 2.0 from steady-state optical absorption spectroscopy (Supporting Information, Figure S3). After cross-linking these NCs with PAE-**1**, $OD_{638\,nm}$:OD_{848nm} increases only slightly to 2.4, but we now find a dramatic increase in $I_{photo,638\,nm}$:$I_{photo,848\,nm}$ to 7 ± 1. This strongly selective photocurrent increase at 638 nm cannot be explained by direct absorption of the organic semiconductor (Supporting Information, Figure S4). Figure 2a displays the time-dependent current output of the same PbS-PAE-**1** hybrid film under a constant bias of + 200 mV and several exposure periods with 638 nm or 848 nm light at the same optical power. The comparison illustrates the ample ON/OFF ratio under 638 nm excitation as well as a roughly seven times smaller ON/OFF ratio for 848 nm as mentioned above. Figure 2b shows the bias-dependence of the ON/OFF ratios for both wavelengths, which exhibit two relative maxima at −6 V and + 0.7 V. While the physical origin of these maxima is not clear, we speculate that here the flat-band condition in the semiconductor material is mostly fulfilled, which leads to minimal OFF currents and, thus, maxima in the ON/OFF ratios.[19] Figure 2c compares the power dependence of the ON/OFF ratio at the two favorable bias values for both excitation wavelengths.

To design a nanoscale optical transistor, we cut a 140 nm × 100 μm channel (length and width, respectively; Figure 2d; Supporting Information, Figure S5) into a thin Au film and cover the channel with a PbS-PAE-**1** film. In Figure 2e, we investigate the photoresponse of the device with a stage-scanning confocal microscope equipped with a 633 nm helium-neon laser after background subtraction.[21] In Figure 2f, we present a comparison of the power-dependent responsivities of the PbS-PAE-**1** film across the nanochannel under 633 nm vs. 488 nm excitation and 0.1 V constant bias as well as the responsivity of the device analyzed in Figure 2a–c under 848 nm light and 0.7 V bias. It is evident that the photoresponse of the PbS-PAE-**1** film deviates severely from the optical absorption spectrum in that the responsivity at 633 nm is about 20 times larger than at 488 nm, although OD_{633nm}:OD_{488nm} is only roughly 0.3. We also attempt to measure the photoresponse under direct excitation of the PAE-**1** singlet transition utilizing a 409 nm laser diode. However, rapid photodegradation and irreversible deterioration of the photocurrent rendered a comparative responsivity performance impossible.

The above findings suggest a greatly altered electronic structure of PbS-PAE-**1** under optical excitation, which we probe by transient absorption (TA) and photoluminescence (PL) spectroscopy. Following the selective photoexcitation of the PbS excitonic transition with 1100 nm pulses, the two-dimensional TA spectrum of PbS-PAE-**1** in Figure 3a displays a broad negative differential absorption (Δ*A*, bleach) near 1200 nm as well as at least two strong bands with positive Δ*A* (induced absorption) between 500–800 nm and a maximum at

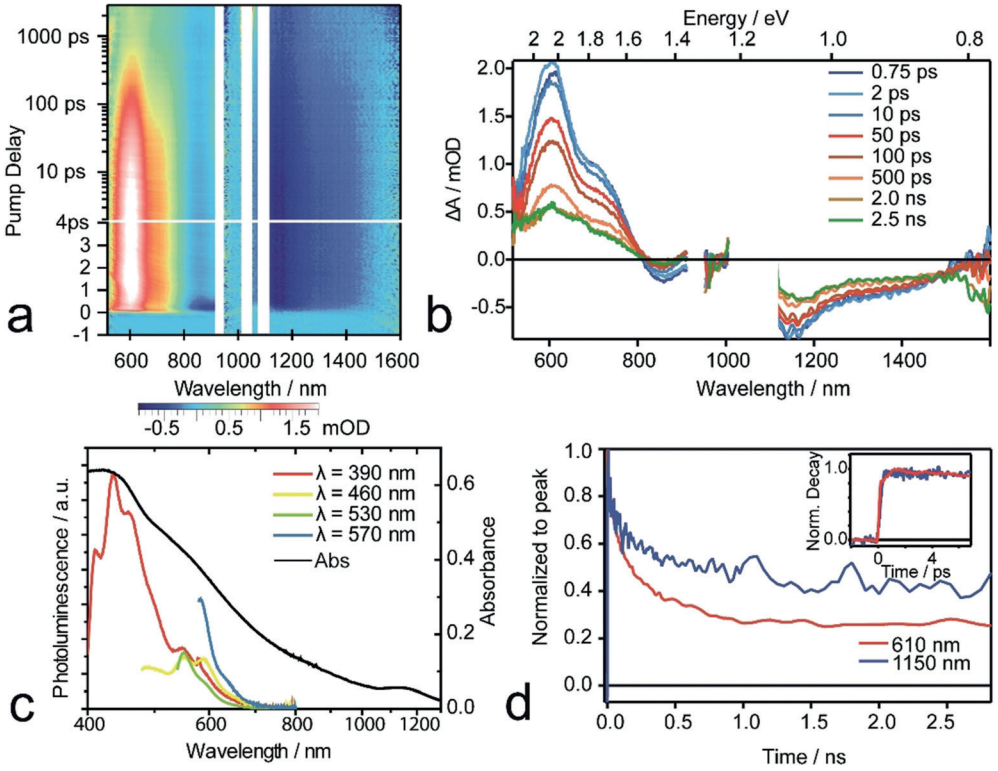

Figure 3. a) Two-dimensional transient absorption spectrum of PbS-PAE-**1** on a quartz substrate, photoexcited with 180 fs laser pulses of 1100 nm. Note that vertical spectral regions are left blank intentionally where detectors were changed and to correct for pump-scatter, the horizontal cut marks the transition from a linear to a semi-logarithmic plot. The color code displays the differential absorption, Δ*A*, where Δ*A* = *A*(excited state) − *A*(ground state). b) Line-cuts through the 2D-spectrum in (a) at different pump delay times. c) Photoluminescence of a PbS-PAE-**1** film on quartz at various excitations. For comparison, the absorption spectrum of the PbS-PAE-**1** film is also displayed (black). d) Temporal decay of the normalized Δ*A* value in the transient absorption spectrum in (a)/(b) at 610 nm vs. 1150 nm. Inset: The same comparison for the first 6 ps of pump–probe delay.

610 nm. This is analyzed in Figure 3b with the display of spectral line cuts through the 2D spectrum in Figure 3a at various pump–probe delay times. While the feature at 1200 nm is attributed to the bleach of the PbS NCs excitonic transition, the shape of the feature at 610 nm is reminiscent of the solid-state absorption of PAE-**1** with vibronic structure[22] (see the Supporting Information, Figure S8 for a comparative measurement of the pure PAE-1 without PbS NCs). In Figure 3c, we investigate the solid-state fluorescence of PbS-PAE-**1** under various excitations between 390–570 nm and find several partially resolved fluorescence bands, which persist even at excitation well below the singlet transition of pure PAE-**1** (for example, at 530 nm). This is further supporting evidence for a modified electronic structure of PAE-**1** upon binding to PbS NCs since pure, solid PAE-**1** exhibits a single, broad fluorescence band centered around 600 nm, which disappears completely upon excitation at 530 nm (Supporting Information, Figure S9). We attribute the induced absorption at 610 nm in PbS-PAE-**1** to the formation of a polaron and note that (O-alkyl)-PAE derivatives are indeed known to exhibit polaronic bands in this spectral region.[23,24] However, activation of these transitions requires direct excitation of the PAE, which is not possible with 1100 nm light. Here, such a polaron could manifest because of charge transfer from the excited PbS NCs onto PAE-**1**. To test this hypothesis, we compare the decay of the optical transition at about 1150 nm with the decay of the polaronic absorption of the polymer in Figure 3d.

We find that both are long-lived (>3 ns) and decay with similar biexponential kinetics (bleach feature at 1150 nm with $\tau_1 = 34 \pm 2$ ps and $\tau_2 = 300 \pm 16$ ps and polaron feature at 610 nm with $\tau_1 = 22 \pm 6$ ps and $\tau_2 = 247 \pm 48$ ps), supporting our hypothesis. We attribute the slightly slower decay of the NC-bleach to the fact that not every photoexcited PbS NC is effectively coupled to a PAE-**1** moiety. We conclude that the reason for the strong photoresponse of PbS-PAE-**1** at 638 nm is most likely the consecutive charge transfer, polaron formation and polaronic absorption in PAE-**1** following the excitation of PbS. In Scheme 1, we illustrate this in terms of the simplified electronic structure at the organic–inorganic interface (left) as well as by idealized representation (right). The relative positions of the energy levels are inferred from reported literature values of the isolated constituents and under the assumption of vacuum-level alignment (−5.0 eV/−4.0 eV for the PbS $1S_h/1S_e$ states and −6.3 to −5.8/−3.6 to −3.9 eV for the HOMO/LUMO of PAE-**1**; all values against vacuum level).[25] The polaron gap ($P_1 \rightarrow P_2$) is reported with 1.9 eV, lifting the P_2 level into close proximity with the $1S_e$ state.[23,24] Scheme 1a marks the charge transfer from an excited NC onto the polymer. This populates the polaronic P_2 level, indicating a charged polymer with altered electronic structure.[26] This charge transfer enforces excited-state absorption from the polaronic ground state (Scheme 1b) and activates the material for absorption of light between 500–800 nm (brown arrow) to result in an excited-state polaron (Scheme 1c). The charge carriers created in this process are mobile owing to the close energetic proximity of the NC levels and contribute to the overall photocurrent.

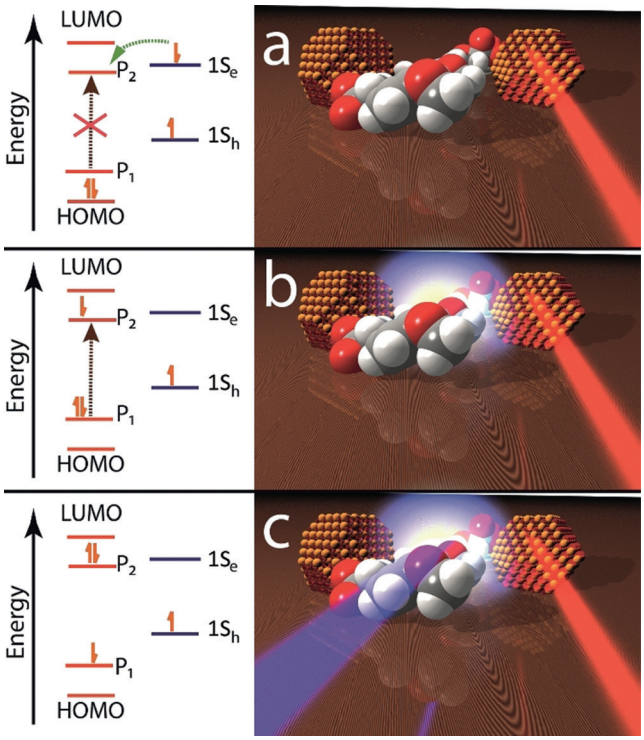

Scheme 1. a) After exciting the $1S_h \rightarrow 1S_e$ transition of the PbS NCs, an electron is transferred (indicated by the green arrow) to the polymer to form a negative polaron (P_2). Before charge transfer, the polaronic levels are unpopulated, such that the polaronic transition has no oscillator strength (marked by the crossed brown arrow). b) Populating the polaron levels increases the oscillator strength of the polaronic transition (brown arrow) and activates the material for absorption at the wavelength of the polaron (indicated by the halo in the idealized picture on the right). c) Excitation of the polaronic transition with a suitable light source creates additional mobile electrons in the polymer, which can readily migrate through the film owing to the close energetic proximity of the $1S_e$ level of the adjacent NCs.

We believe that the concept exemplified here at the PbS-PAE-**1** interface may be generally applicable to different NC-polymer combinations, which allows the optical response of a material to be sensitized with the aid of a second optical stimulus of different frequency. In this sense, the photoresponse of PbS-PAE-**1** to a weak optical stimulus of 500–800 nm is readily amplified by a trigger signal of 1100–1400 nm, which generates the polaron that dramatically increases the oscillator strength for the visible optical stimulus. This concept is of interest for optical communication, for instance in optical switches capable of a single-component AND logic, which requires two specific optical inputs to generate a positive electrical output.

Experimental Section

PbS nanocrystals were synthesized according to established methods, and PAE-**1** synthesized as described in the Supporting Information (see Figure S10 for the structural formula).[27] Hybrid thin films of the two constituents were assembled at the liquid–nitrogen interface following a previously described procedure (for details, see the Supporting Information).[16] The fabrication of the

nanochannels as well as the set-ups utilized for transport-, photocurrent-, transient absorption, and photoluminescence measurement are given in the Supporting Information.

Acknowledgements

J.L. acknowledges funding by Toyota Motor Europe and M.S. thanks the DFG for support under grant SCHE1905/3 and SCHE1905/4. Access to a Horiba Jobin Yvon Labram HR 800 Raman spectrometer granted by Frank Schreiber is gratefully acknowledged.

Keywords: conductive polymers · coupled organic–inorganic nanostructures · photoswitches · polarons

How to cite: *Angew. Chem. Int. Ed.* **2018**, *57*, 11559–11563
Angew. Chem. **2018**, *130*, 11733–11737

[1] M. Smit, J. van der Tol, M. Hill, *Laser Photonics Rev.* **2012**, *6*, 1–13.
[2] D. Thomson, A. Zilkie, J. E. Bowers, T. Komljenovic, G. T. Reed, L. Vivien, D. Marris-Morini, E. Cassan, L. Virot, J.-M. Fédéli, et al., *J. Opt.* **2016**, *18*, 073003.
[3] a) T. D. Anthopoulos, *Appl. Phys. Lett.* **2007**, *91*, 113513; b) J. K. Marmon, S. C. Rai, K. Wang, W. Zhou, Y. Zhang, *Front. Phys.* **2016**, *4*, 8; c) K. S. Narayan, N. Kumar, *Appl. Phys. Lett.* **2001**, *79*, 1891.
[4] D. A. B. Miller, *Appl. Opt.* **2010**, *49*, F59–F70.
[5] a) W. Heni, Y. Kutuvantavida, C. Haffner, H. Zwickel, C. Kieninger, S. Wolf, M. Lauermann, Y. Fedoryshyn, A. F. Tillack, L. E. Johnson, et al., *ACS Photonics* **2017**, *4*, 1576–1590; b) F. H. L. Koppens, T. Mueller, P. Avouris, A. C. Ferrari, M. S. Vitiello, M. Polini, *Nat. Nanotechnol.* **2014**, *9*, 780–793; c) D. Kufer, G. Konstantatos, *ACS Photonics* **2016**, *3*, 2197–2210; d) S. Masala, V. Adinolfi, J.-P. Sun, S. D. Gobbo, O. Voznyy, I. J. Kramer, I. G. Hill, E. H. Sargent, *Adv. Mater.* **2015**, *27*, 7445–7450.
[6] D. Kufer, I. Nikitskiy, T. Lasanta, G. Navickaite, F. H. L. Koppens, G. Konstantatos, *Adv. Mater.* **2015**, *27*, 176–180.
[7] G. Konstantatos, M. Badioli, L. Gaudreau, J. Osmond, M. Bernechea, de Arquer, F. Pelayo Garcia, F. Gatti, F. H. L. Koppens, *Nat. Nanotechnol.* **2012**, *7*, 363–368.
[8] a) P. Gu, Y. Yao, L. Feng, S. Niu, H. Dong, *Polym. Chem.* **2015**, *6*, 7933–7944; b) Y.-Y. Noh, D.-Y. Kim, K. Yase, *J. Appl. Phys.* **2005**, *98*, 074505; c) Y.-Y. Noh, D.-Y. Kim, Y. Yoshida, K. Yase, B.-J. Jung, E. Lim, H.-K. Shim, *Appl. Phys. Lett.* **2005**, *86*, 043501.
[9] V. Adinolfi, I. J. Kramer, A. J. Labelle, B. R. Sutherland, S. Hoogland, E. H. Sargent, *ACS Nano* **2015**, *9*, 356–362.
[10] a) V. Adinolfi, E. H. Sargent, *Nature* **2017**, *542*, 324–327; b) W. Peng, S. Sampat, S. M. Rupich, B. Anand, H. M. Nguyen, D. Taylor, B. E. Beardon, Y. N. Gartstein, Y. J. Chabal, A. V. Malko, *Nanoscale* **2015**, *7*, 8524–8530.
[11] C. Livache, E. Izquierdo, B. Martinez, M. Dufour, D. Pierucci, S. Keuleyan, H. Cruguel, L. Becerra, J. L. Fave, H. Aubin, et al., *Nano Lett.* **2017**, *17*, 4067–4074.
[12] T. Aqua, R. Naaman, A. Aharoni, U. Banin, Y. Paltiel, *Appl. Phys. Lett.* **2008**, *92*, 223112.
[13] a) A. Neubauer, S. Yochelis, Y. Amit, U. Banin, Y. Paltiel, *Sens. Actuators A* **2015**, *229*, 166–171; b) S. Yang, N. Zhao, L. Zhang, H. Zhong, R. Liu, B. Zou, *Nanotechnology* **2012**, *23*, 255203.
[14] H. Zhang, Y. Zhang, X. Song, Y. Yu, M. Cao, Y. Che, Z. Zhang, H. Dai, J. Yang, G. Zhang, et al., *ACS Photonics* **2017**, *4*, 584–592.
[15] a) S. Bhattacharyya, A. Patra, *J. Photochem. Photobiol. C* **2014**, *20*, 51–70; b) A. A. Lutich, G. Jiang, A. S. Susha, A. L. Rogach, F. D. Stefani, J. Feldmann, *Nano Lett.* **2009**, *9*, 2636–2640; c) F. S. F. Morgenstern, A. Rao, M. L. Böhm, R. J. P. Kist, Y. Vaynzof, N. C. Greenham, *ACS Nano* **2014**, *8*, 1647–1654; d) E. Strein, D. W. deQuilettes, S. T. Hsieh, A. E. Colbert, D. S. Ginger, *J. Phys. Chem. Lett.* **2014**, *5*, 208–211.
[16] A. André, C. Theurer, J. Lauth, S. Maiti, M. Hodas, M. Samadi Khoshkhoo, S. Kinge, A. J. Meixner, F. Schreiber, L. D. A. Siebbeles, et al., *Chem. Commun.* **2017**, *53*, 1700–1703.
[17] G. Konstantatos, I. Howard, A. Fischer, S. Hoogland, J. Clifford, E. Klem, L. Levina, E. H. Sargent, *Nature* **2006**, *442*, 180–183.
[18] a) J.-S. Lee, M. V. Kovalenko, J. Huang, D. S. Chung, D. V. Talapin, *Nat. Nanotechnol.* **2011**, *6*, 348–352; b) Y. Zhang, D. J. Hellebusch, N. D. Bronstein, C. Ko, D. F. Ogletree, M. Salmeron, A. P. Alivisatos, *Nat. Commun.* **2016**, *7*, 11924.
[19] P. Nagpal, V. I. Klimov, *Nat. Commun.* **2011**, *2*, 486.
[20] J. P. Clifford, G. Konstantatos, K. W. Johnston, S. Hoogland, L. Levina, E. H. Sargent, *Nat. Nanotechnol.* **2009**, *4*, 40–44.
[21] T. Zuechner, A. V. Failla, A. Hartschuh, A. J. Meixner, *J. Microsc.* **2008**, *229*, 337–343.
[22] a) U. H. F. Bunz, J. M. Imhof, R. K. Bly, C. G. Bangcuyo, L. Rozanski, D. A. Vanden Bout, *Macromolecules* **2005**, *38*, 5892–5896; b) F. Feng, J. Yang, D. Xie, T. D. McCarley, K. S. Schanze, *J. Phys. Chem. Lett.* **2013**, *4*, 1410; c) F. Panzer, H. Bässler, A. Köhler, *J. Phys. Chem. Lett.* **2017**, *8*, 114–125; d) M. I. Sluch, A. Godt, U. H. F. Bunz, M. A. Berg, *J. Am. Chem. Soc.* **2001**, *123*, 6447–6448.
[23] C. Enengl, S. Enengl, N. Bouguerra, M. Havlicek, H. Neugebauer, D. A. M. Egbe, *ChemPhysChem* **2017**, *18*, 93–100.
[24] X. M. Jiang, C. C. Wu, M. Wohlgenannt, W. Y. Huang, T. K. Kwei, Y. Okamoto, Z. V. Vardeny, *Physica B Condens. Matter* **2003**, *338*, 235–239.
[25] a) S. Axnanda, M. Scheele, E. Crumlin, B. Mao, R. Chang, S. Rani, M. Faiz, S. Wang, A. P. Alivisatos, Z. Liu, *Nano Lett.* **2013**, *13*, 6176–6182; b) J. Jasieniak, M. Califano, S. E. Watkins, *ACS Nano* **2011**, *5*, 5888–5902; c) A. Montali, P. Smith, C. Weder, *Synth. Met.* **1998**, *97*, 123–126; d) D. Ofer, T. M. Swager, M. S. Wrighton, *Chem. Mater.* **1995**, *7*, 418–425.
[26] a) J. L. Bredas, G. B. Street, *Acc. Chem. Res.* **1985**, *18*, 309–315; b) S. Fratiloiu, F. C. Grozema, L. D. A. Siebbeles, *J. Phys. Chem. B* **2005**, *109*, 5644–5652; c) G. Heimel, *ACS Cent. Sci.* **2016**, *2*, 309–315; d) S. Winkler, P. Amsalem, J. Frisch, M. Oehzelt, G. Heimel, N. Koch, *Mater. Horiz.* **2015**, *2*, 427–433.
[27] M. C. Weidman, M. E. Beck, R. S. Hoffman, F. Prins, W. A. Tisdale, *ACS Nano* **2014**, *8*, 6363–6371.

Manuscript received: March 21, 2018
Accepted manuscript online: July 1, 2018
Version of record online: August 1, 2018

